Editors' Suggestion

Shortcuts to Equilibrium with a Levitated Particle in the Underdamped Regime

Damien Raynal,[1] Timothée de Guillebon,[1] David Guéry-Odelin,[2] Emmanuel Trizac,[3,4] Jean-Sébastien Lauret,[1] and Loïc Rondin[1,*]

[1]Université Paris-Saclay, ENS Paris-Saclay, CNRS, CentraleSupélec, LuMIn, 91405 Orsay Cedex, France
[2]Université Paul Sabatier–Toulouse 3, CNRS, LCAR, 31062 Toulouse Cedex 9, France
[3]Université Paris-Saclay, CNRS, LPTMS, 91405 Orsay Cedex, France
[4]Univ Lyon, ENS de Lyon, F-69342 Lyon, France

(Received 4 January 2023; accepted 24 July 2023; published 25 August 2023)

We report on speeding-up equilibrium recovery in the previously unexplored general case of the underdamped regime using an optically levitated particle. We accelerate the convergence toward equilibrium by an order of magnitude compared to the natural relaxation time. We then discuss the efficiency of the studied protocols, especially for a multidimensional system. These results pave the way for optimizing realistic nanomachines with application to sensing and developing efficient nanoheat engines.

DOI: 10.1103/PhysRevLett.131.087101

In the quest to achieve better control over physical systems in the classical, quantum, and stochastic realms, the ability to perform transformations between equilibrium states is paramount. The opportunity to realize such transformations at high speed could then improve the system's efficiency. For instance, in the context of stochastic thermodynamics, shortcuts to equilibrium protocols have been proposed to optimize force sensors [1], nanoheat engines [2], or computing [3]. These applications have triggered significant works devoted to one-dimensional shortcut protocols, where the relaxation path of the system is designed to reach equilibrium in an arbitrarily short time t_f, faster than the natural relaxation time t_{relax} that governs the time evolution after a sudden change of the system parameters [4–8]. For instance, protocols accelerating isothermal compression and expansion have been experimentally demonstrated for overdamped systems [2,5,9]. However, to understand the fundamental nature of the shortcuts to equilibrium protocols, one must address the more general underdamped regime, where the inertia of the system cannot be neglected and for which the position, the velocity, and their correlation must be taken into account [6,10]. The underdamped regime gives access to nonthermal states, that are ideally suited for studying nonequilibrium fluctuations for transitions between arbitrary steady states [11]. It also provides equilibrium information from nonequilibrium measurements [12], and is essential for temperature-changing transitions [13,14]. Beyond these fundamental questions, extending shortcuts to equilibrium to the underdamped regime is also essential to improve nanomechanical systems that usually operate in this regime, or to take advantage of the control that one can enforce on weakly damped systems, and which may lead, for example, to the development of all-optical nanoheat-engines [15]. A first step toward answering this question has been taken with the demonstration of accelerated transport protocols using an underdamped micromechanical oscillator [1]. Nevertheless, in this one-dimensional example, only the average system position is engineered, and the resulting protocol is oblivious to fluctuations. More subtle protocols are required in general to control the system's position and velocity standard deviations simultaneously, including more spatial dimensions. This is a much harder task, which should take into account fluctuations and the coupling between degrees of freedom [10]. In that context, extending the experimentally underdamped shortcut to equilibrium to more general protocols can benefit from the recent developments on optically levitated particles [16–18], which provide excellent tools to track particle dynamics and where the system damping can be easily tuned [19].

In this Letter, we implement the first experimental acceleration of a harmonic expansion in the underdamped regime. We also demonstrate that accurate measurement of levitated nanoparticles' position and velocity makes it perfectly fitted to monitor the out-of-equilibrium dynamics of stochastic systems, by allowing the easy following of dynamics in the entire phase space, which is not the case in the overdamped regime. Finally, we discuss the robustness of shortcuts to equilibrium protocols by studying the particle relaxation for its different degrees of freedom.

Figure 1 shows a sketch of the experimental setup. A 73 nm silica particle is trapped by optical tweezers made from a high-power near-infrared (NIR) laser beam. The particle dynamics is measured with a common path interferometer using an ancillary green laser beam and a quadrant photodetector [20]. The potential experienced by the particle is well approximated by a 3D harmonic potential, whose transverse trap stiffness k^x_{trap} can be modified by changing the light intensity of the tweezers.

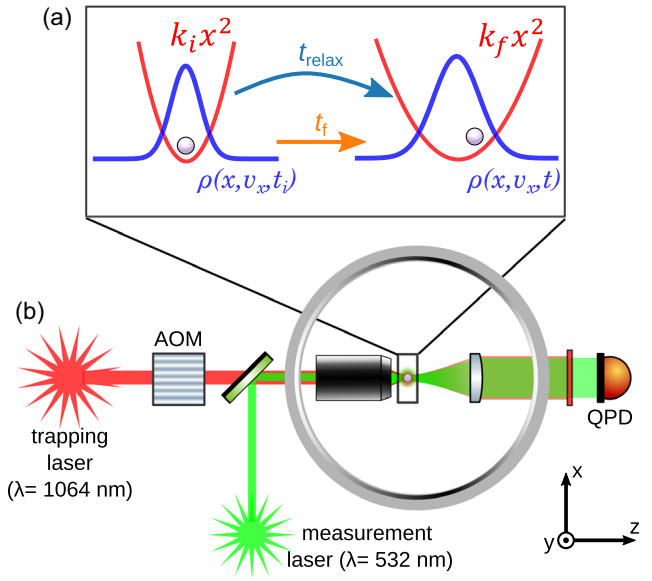

FIG. 1. (a) Shortcut to equilibration for a trap expansion. The trap stiffness is changed from k_i to k_f. Using shortcut protocols, the equilibrium is reached in a target time t_f shorter than the natural relaxation time of the system t_{relax}. The equilibration dynamics can be tracked through the probability distribution function $\rho(x, v_x, t)$. (b) A NIR laser beam traps a silica nanoparticle at the focus of a high-NA microscope objective. The NIR laser power is controlled with an AOM (acousto-optic modulator). The particle dynamics is measured with a green laser and a quadrant photodiode.

We study an expansion of the potential corresponding to a change of the trap stiffness from k_i to $k_f < k_i$. The objective is to develop a protocol acting on a control parameter of the system, here the trap stiffness, to accelerate the equilibration of the system in a chosen time t_f, shorter than the system's natural relaxation time t_{relax}. The three eigenangular frequencies of the harmonic trapping are nondegenerate. We measure $\omega_x/2\pi \approx 300$ kHz, $\omega_y/2\pi \approx 250$ kHz, and $\omega_z/2\pi \approx 90$ kHz. The trap stiffness along each of these axes $q = \{x, y, z\}$ is $k^q_{\mathrm{trap}} = m\omega_q^2$, where m is the particle mass; it is then directly proportional to the NIR trapping laser power P_{las} [20]. Using an acousto-optic modulator, we can dynamically tune P_{las} and thus finely control the trap stiffness. The trapping setup is enclosed inside a vacuum chamber to control the particle's interaction with its environment. Indeed, the system damping rate Γ is directly proportional to the gas pressure p_{gas} inside the chamber [19]. Here, we are specifically interested in the underdamped regime. Thus, we set a gas pressure of $p_{\mathrm{gas}} = 5$ hPa, corresponding to a reduced damping rate $\Gamma/2\pi \approx 3$ kHz, such that the underdamped condition $\Gamma < \omega_q$ is fulfilled for the three axes $q = \{x, y, z\}$ [21]. Nevertheless, note that our experimental setup allows us to readily extend the presented work to a wide range of damping rates, and notably to the overdamped regime [21]. More details about the experimental setup can be found in [21].

To determine the natural relaxation time of the system t_{relax}, we perform a STEP protocol, consisting of an instantaneous change in the trap stiffness k_{trap} from an initial value k_i to a final value k_f, as shown in Fig. 2(a). We introduce the compression factor $\chi = k_f/k_i$. In the following, we focus on the case of isothermal expansion $\chi < 1$, while our experimental setup can also naturally address isothermal compressions [21]. We study the dynamics of the particle along the x axis over a set of 2×10^4 isothermal expansions with $\chi = 0.6$. Interestingly, the good signal-to-noise ratio of our measurement scheme allows us to determine the particle velocity v_x from a point-by-point derivative of x. We thus study the particle relaxation after the STEP protocol by computing the standard deviation in position σ_x and velocity σ_{v_x}, as shown in Figs. 2(b) and 2(c). These data exhibit a couple of interesting features. First, at equilibrium, we observe steady-state values $\sigma^{\mathrm{eq}}_{x,\{i,f\}} = \sqrt{k_B T/k_{\{i,f\}}}$ and $\sigma^{\mathrm{eq}}_{v_x} = \sqrt{k_B T/m}$ as expected from the equipartition theorem. Besides, contrasting with the overdamped case [2,5], we observe in the transient regime damped oscillations in phase oppositions for σ_x and σ_{v_x}. These oscillations can be seen as a coherent exchange of the system's average potential and kinetic energy, in analogy with a classical underdamped harmonic oscillator. Finally, from a fit to the analytical solution, we confirm that in the strongly underdamped regime achieved here ($\Gamma \ll \omega_f$), the oscillation frequency is twice the natural trap frequency, $\omega_{\mathrm{relax}} = 2\omega_{x,f} = 2\pi \times 519$ kHz and that the system's characteristic relaxation time is given by the velocity relaxation time $t_{\mathrm{relax}} = t_v = 1/\Gamma = 43$ μs, leading to a STEP equilibration in a time close to $3t_{\mathrm{relax}}$ (i.e., σ_x and σ_{v_x} reached 95% of their equilibrium values) [21].These observations starkly contrast with previous overdamped experiments, where the system thermalizes instantaneously with the environment, and in which the limiting timescale is given by the position relaxation time $t_x = \Gamma/\omega^2$ necessary for the nanoparticle to explore the new potential [2,5]. They thus highlight the importance of addressing the underdamped regime to fully capture the nature of nanosystems.

Once this natural relaxation time is measured, we focus on shortcutting the system equilibration time. In that context, the theoretical proposal by Chupeau *et al.* [10] is particularly interesting. Indeed, it extends the engineering of swift equilibration (ESE), initially developed for overdamped systems, to the underdamped regime. The idea behind this ESE formalism is to find a probability density function $\rho(x, v_x, t)$ that is a solution of the Fokker-Planck equation describing the dynamics of the particle,

$$\frac{\partial \rho}{\partial t} + v_x \frac{\partial \rho}{\partial x} - \frac{k^x_{\mathrm{trap}}}{m} x \frac{\partial \rho}{\partial v_x} = \frac{\Gamma}{m} \frac{\partial v_x \rho}{\partial v_x} + \frac{\Gamma k_B T}{m^2} \frac{\partial^2 \rho}{\partial v_x^2}, \qquad (1)$$

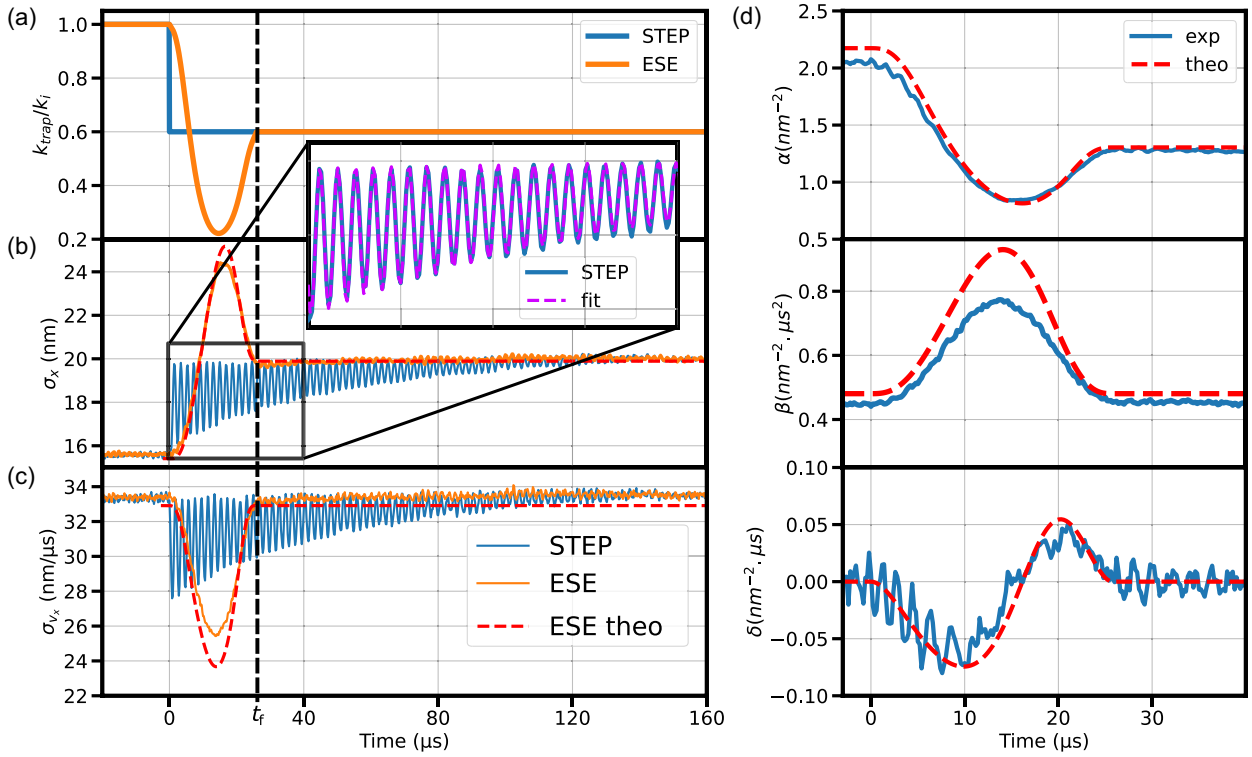

FIG. 2. (a) Evolution of the trap stiffness for a harmonic expansion in the case of a STEP protocol (blue) and the accelerating ESE protocol described in the main text (orange). (b) and (c) Evolution of the standard deviation in position σ_x (b) and velocity σ_{v_x} (c) for the STEP (blue) and the ESE protocol (orange) presented in (a). The black dotted vertical line corresponds to the final time $t_f = 26$ μs of the ESE protocol. Dashed red lines are the expected theoretical values for σ_x and σ_{v_x} Inset: close-up view of σ_x highlighting the oscillations. A fit (dashed purple line) provides the value of $\omega_{\text{relax}}/2\pi = 519 \pm 1$ kHz and $\Gamma/2\pi = 3.1 \pm 0.2$ kHz. (d) Evolution of α, β, and δ (as defined in text) during the out-of-equilibrium regime of the ESE protocol pictured in (a). The experimental values (blue) are compared with those calculated for the ESE protocol (dashed red lines).

and that reaches the final aimed equilibrium state in an arbitrary small finite time t_f. To this end, and by virtue of the linearity of the applied force, one may search for a Gaussian solution of the form

$$\rho(x, v_x, t) = N(t) \exp\{-[\alpha(t)x^2 + \beta(t)v_x^2 + \delta(t)xv_x]\}, \tag{2}$$

where α, β, and δ are functions to be determined, and N is a normalization factor [21]. Solving this problem provides a continuous-time evolution of the trap stiffness $k^x_{\text{trap}}(t)$ as the control parameter of the system equilibration. For example, we depict in Fig. 2(a), the trap stiffness evolution we compute for an ESE protocol corresponding to a fivefold acceleration over the nominal equilibration time $3t_{\text{relax}} = 129$ μs, and to a protocol duration $t_f = 26$ μs.

Applying this ESE protocol to our particle leads to the evolution of the standard deviations σ_x and σ_{v_x} shown in orange in Figs. 2(b) and 2(c). We verify that the system's relaxation is actually shortened and that both position and velocity variances reach their equilibrium values exactly at the protocol's final time $t_f = 26$ μs (black dotted line in Fig. 2). Furthermore, our ability to measure both x and v_x allows us to fully monitor the probability distribution function. Specifically, we can compute from these data the values of α, β, and δ during the protocol. As shown in Fig. 2(d), we observe a good agreement with the theoretical target functions enforced by the protocol, demonstrating the power of the ESE approach to engineer equilibration [21]. We also stress that the ESE strategy is a full feed-forward approach. Thus, conversely to feedback, its efficiency does not rely on the knowledge on the particle real-time dynamics.

These results are thus the first demonstration of accelerated equilibration of a particle in the underdamped regime. They stress that trap stiffness can be used as a single experimental control parameter acting on both position and velocity to design shortcuts protocols. They also show that we can fully measure and reconstruct the evolution of the distribution of probability $\rho(x, v_x, t)$ during state-to-state transformations, highlighting levitated particles as a perfect system for out-of-equilibrium studies. Besides, within our approach, the set of admissible controls is infinite. Here, we focus on shortcuts to equilibrium, but other protocols targeting minimum entropy production and

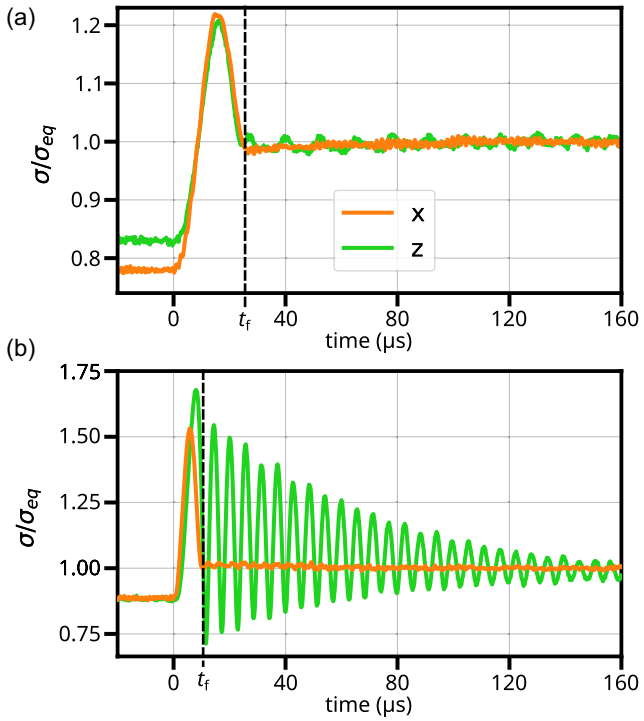

FIG. 3. Evolution of the position standard deviation σ, normalized by its final equilibrium value σ_{eq}, along the x axis (orange) and z axis (green) during an ESE protocol defined on the x axis at the frequency $\omega_{x,i}/2\pi = 340$ kHz, and with $\omega_z \approx \omega_x/3.4$. (a) Equilibration for a fivefold accelerating equilibration protocol for a $\chi = 0.6$ expansion. (b) Equilibration for a 17-fold accelerating equilibration protocol for a $\chi = 0.75$ expansion. The black dotted vertical lines correspond to the final times $t_f = 26$ μs (a) $t_f = 7.75$ μs (b) of the two ESE protocols.

dissipation [22,24] or mean work provided by the operator [25] could also be addressed. Characterizing such protocols requires retrieving the heat and work exchanged by the particle to the environment. Knowing the dynamics of the levitated particle, it is information that we can retrieve [21].

Beyond accelerating equilibration, a natural question related to ESE protocols is their resilience to changes or uncertainties in the system's parameters. Of particular interest is the design of robust protocols that shorten equilibration of a set of oscillators at different frequencies. Indeed, this could provide protocols insensitive to frequency fluctuations [26] or able to address systems with multiple degrees of freedom, such as arrays of oscillators [8], Brownian gyrators [27,28], or multimode oscillators [1].

To test the robustness of the ESE protocols in our specific case, we take advantage of the three-dimensional nature of our system. Indeed, the three normal modes are nondegenerate and uncoupled to first order. Recording the three-dimensional dynamics of the particle allows us to study the system equilibration along different axes, corresponding to uncoupled oscillators at different frequencies undergoing the same relative stiffness evolution. Specifically, we focus on comparing x and z axes that represent the largest frequency mismatch in our experiment $\omega_x/\omega_z \approx 3.4$. We thus apply the ESE protocols studied previously and designed for the x axis (Fig. 2). To study the relaxation of each axis, we compute the standard deviation for the particle position along these x and z axes. As shown in Fig. 3(a), for this fivefold accelerated equilibration, the protocol designed for the x axis works surprisingly well for the lower frequency z axis, which also reaches equilibrium at the final protocol time $t_f = 26$ μs. Note that similar results are also observed for the relaxation along the y axis, that is at a natural frequency ω_y close from the one of the x axis $\omega_x \approx 1.3\omega_y$ [21].

To push the limits of the robustness of the ESE protocols, we have also designed a faster protocol with a final time $t_f = 7.75$ μs, corresponding to a 17-fold accelerated equilibration compared to natural relaxation. The faster protocols are more demanding in terms of required total laser power. Because of experimental constraints, we thus reduce the expansion factor of the protocol to $\chi = 0.75$. Figure 3(b) shows the corresponding relaxation of the standard deviation of position along x and z. First, we verify that the protocol is efficient for the design axis (x axis), and that σ_x actually reaches its steady state value at the protocol's final time $t_f = 7.75$ μs (black dotted line in the figure). We thus demonstrate that ESE protocols applied to a single oscillator can achieve equilibration accelerated by more than an order of magnitude in the underdamped regime. Conversely, along the z axis, the protocol drives the system out of equilibrium. After the protocol final time $t = t_f$, the system thus relaxes to equilibrium, dissipating its extra energy to the bath, as observed for STEP protocols in Fig. 2. We therefore observe oscillations of the position standard deviation σ_z at the frequency $2\omega_{z,f}$ with a characteristic relaxation time $t_v = 1/\Gamma$.

Hence, we observe that for moderate equilibration acceleration, ESE protocols are resilient to changes in frequency. We can engineer equilibrium states even far from the target frequency. When the protocol speed is increased, this property becomes harder to meet. For the fastest protocols studied here, to observe an efficient equilibration, the actual system frequency must match the one of the protocol within a few percent [21].

To conclude, we have shown that engineering swift equilibration can be successfully applied in the underdamped regime. We demonstrate accelerated equilibration by more than an order of magnitude for expansion protocols for a single frequency oscillator, and intermediate speedup for a multidimensional one. In addition, we highlight that by using optically levitated particles, we can reconstruct the particle's dynamics, providing complete information about the system's probability density function. Taking advantage of the levitated particle's different degrees of freedom, we also address our shortcuts to equilibrium protocols' robustness. Finally, we report that

moderate acceleration can be applied to oscillators with a broad frequency range. Our Letter paves the way for developing generic state-to-state protocols and discussing the fundamental physical limits of shortcuts to equilibrium protocols' robustness. Thus, future works may include fast multidimensional shortcuts, taking advantage of the vast space of relaxation paths offered by ESE-like protocols [6,7,10,28] or by optimal control theory framework [29]. Also, by taking advantage of the recent developments of thermal bath engineering [30,31] and fine temperature control [32,33] of levitated particles, a natural extension rests in the use of shortcuts to equilibrium and optimal protocols for the optimization of power and efficiency of nanoheat engines [15].

This work is supported by the Investissements d'Avenir of LabEx PALM (ANR-10-LABX-0039-PALM), and by the ANR projects OPLA (ANR-20-CE30-0014) and STATE (ANR-18-CE30-0013). We thank C. Lopez and S. L'Horset for support with electronics, F. Bretenaker for lending a laser, H. Huet and B. Gebel for seminal experimental work, and M. Baldovin, L. Bellon, S. Ciliberto, S. Dago, C. Plata together with A. Prados for useful discussions.

*loic.rondin@universite-paris-saclay.fr

[1] A. Le Cunuder, I. A. Martínez, A. Petrosyan, D. Guéry-Odelin, E. Trizac, and S. Ciliberto, Appl. Phys. Lett. **109**, 113502 (2016).
[2] J. A. C. Albay, P.-Y. Lai, and Y. Jun, Appl. Phys. Lett. **116**, 103706 (2020).
[3] A. B. Boyd, A. Patra, C. Jarzynski, and J. P. Crutchfield, J. Stat. Phys. **187**, 17 (2022).
[4] D. Guéry-Odelin, A. Ruschhaupt, A. Kiely, E. Torrontegui, S. Martínez-Garaot, and J. G. Muga, Rev. Mod. Phys. **91**, 045001 (2019).
[5] I. A. Martínez, A. Petrosyan, D. Guéry-Odelin, E. Trizac, and S. Ciliberto, Nat. Phys. **12**, 843 (2016).
[6] G. Li, H. T. Quan, and Z. C. Tu, Phys. Rev. E **96**, 012144 (2017).
[7] M. Chupeau, B. Besga, D. Guéry-Odelin, E. Trizac, A. Petrosyan, and S. Ciliberto, Phys. Rev. E **98**, 010104 (2018).
[8] S. Dago, B. Besga, R. Mothe, D. Guéry-Odelin, E. Trizac, A. Petrosyan, L. Bellon, and S. Ciliberto, SciPost Phys. **9**, 064 (2020).
[9] Y. Rosales-Cabara, G. Manfredi, G. Schnoering, P.-A. Hervieux, L. Mertz, and C. Genet, Phys. Rev. Res. **2**, 012012 (2020).
[10] M. Chupeau, S. Ciliberto, D. Guéry-Odelin, and E. Trizac, New J. Phys. **20**, 075003 (2018).
[11] J. Gieseler, R. Quidant, C. Dellago, and L. Novotny, Nat. Nanotechnol. **9**, 358 (2014).
[12] G. Li and Z. C. Tu, Phys. Rev. E **103**, 032146 (2021).
[13] I. A. Martínez, É. Roldán, L. Dinis, D. Petrov, and R. A. Rica, Phys. Rev. Lett. **114**, 120601 (2015).
[14] Y. Jun and P.-Y. Lai, Phys. Rev. Res. **3**, 033130 (2021).
[15] A. Dechant, N. Kiesel, and E. Lutz, Phys. Rev. Lett. **114**, 183602 (2015).
[16] C. Gonzalez-Ballestero, M. Aspelmeyer, L. Novotny, R. Quidant, and O. Romero-Isart, Science **374**, eabg3027 (2021).
[17] M. A. Ciampini, T. Wenzl, M. Konopik, G. Thalhammer, M. Aspelmeyer, E. Lutz, and N. Kiesel, arXiv:2107.04429.
[18] J. Gieseler and J. Millen, Entropy **20**, 326 (2018).
[19] L. Rondin, J. Gieseler, F. Ricci, R. Quidant, C. Dellago, and L. Novotny, Nat. Nanotechnol. **12**, 1130 (2017).
[20] J. Gieseler, B. Deutsch, R. Quidant, and L. Novotny, Phys. Rev. Lett. **109**, 103603 (2012).
[21] See Supplemental Material at http://link.aps.org/supplemental/10.1103/PhysRevLett.131.087101, which includes Refs. [10,13,20,22,23], for details about experimental methods, calculation, and modeling of the system dynamics during step and ESE protocols and for supplemental figures.
[22] P. Muratore-Ginanneschi and K. Schwieger, Phys. Rev. E **90**, 060102(R) (2014).
[23] C. Zerbe, P. Jung, and P. Hänggi, Phys. Rev. E **49**, 3626 (1994).
[24] P. Muratore-Ginanneschi, J. Stat. Mech. (2014) P05013.
[25] A. Gomez-Marin, T. Schmiedl, and U. Seifert, J. Chem. Phys. **129**, 024114 (2008).
[26] M. Sansa, E. Sage, E. C. Bullard, M. Gély, T. Alava, E. Colinet, A. K. Naik, L. G. Villanueva, L. Duraffourg, M. L. Roukes, G. Jourdan, and S. Hentz, Nat. Nanotechnol. **11**, 552 (2016).
[27] A. Baldassarri, A. Puglisi, and L. Sesta, Phys. Rev. E **102**, 030105 (2020).
[28] A. G. Frim, A. Zhong, S.-F. Chen, D. Mandal, and M. R. DeWeese, Phys. Rev. E **103**, L030102 (2021).
[29] V. Martikyan, D. Guéry-Odelin, and D. Sugny, Phys. Rev. A **101**, 013423 (2020).
[30] A. Militaru, M. Innerbichler, M. Frimmer, F. Tebbenjohanns, L. Novotny, and C. Dellago, Nat. Commun. **12**, 2446 (2021).
[31] M. Rademacher, M. Konopik, M. Debiossac, D. Grass, E. Lutz, and N. Kiesel, Phys. Rev. Lett. **128**, 070601 (2022).
[32] L. Magrini, P. Rosenzweig, C. Bach, A. Deutschmann-Olek, S. G. Hofer, S. Hong, N. Kiesel, A. Kugi, and M. Aspelmeyer, Nature (London) **595**, 373 (2021).
[33] F. Tebbenjohanns, M. L. Mattana, M. Rossi, M. Frimmer, and L. Novotny, Nature (London) **595**, 378 (2021).